

A method to estimate the lateral tire force and the sideslip angle of a vehicle: Experimental validation

Moustapha Doumiati, Alessandro Victorino, Ali Charara and Daniel Lechner

Abstract—The motion of a vehicle is governed by the forces generated between the tires and the road. Knowledge of these dynamic variables is important for vehicle control systems that aim to enhance vehicle stability and passenger safety. Unfortunately, it is difficult to obtain these data because of technical and economic reasons, therefore, they must be estimated. This study introduces a new estimation process for lateral tire/road forces and vehicle's sideslip angle. The proposed method presents many benefits over the existing state-of-art works, within the dynamic estimation framework. One of these major contributions consists of evaluating the lateral tire forces at each tire and not per axle. The proposed estimation method is derived from the Extended Kalman filter and is based on the dynamic response of a vehicle instrumented with potentially integrable sensors. The performance of this concept is tested and compared to real experimental data using a laboratory car. Experimental results show that the proposed approach is a promising technique to provide accurate estimations of vehicle dynamic states.

I. INTRODUCTION

Today, automotive electronic technologies are being developed for safe and comfortable travelling of drivers and passengers. There are a lot of vehicle ADAS (Advanced Driver Assistance Systems) control systems such as Rollover Prevention System, Anti-lock Brake System (ABS), Electronic Stability Control (ESC) and so on. These control systems equipment rate is increasing all around the world. Vehicle control algorithms have made great strides towards improving the handling and the safety of vehicles. For example, experts estimate that ESC prevents 27% of loss-of-control accidents by intervening when emergency situations are detected [1]. While nowadays vehicle control algorithms are undoubtedly a life-saving technology, they are limited by the available vehicle state information.

Vehicle control systems currently available on production cars rely on available inexpensive measurements such as longitudinal velocity, accelerations and yaw rate. However, other essential parameters for improving vehicle safety and handling, such as tire/road forces, are more difficult to measure because of technical and economic reasons. Therefore, these important data must be observed or estimated. This study focuses especially on the estimation of the lateral tire/road forces.

The lateral tire force (also known as side or cornering force)

M. Doumiati, A. Victorino and A. Charara are with Heudiasyc Laboratory, UMR CNRS 6599, Université de Technologie de Compiègne, 60205 Compiègne, France mdoumat@hds.utc.fr, acorrea@hds.utc.fr and acharara@hds.utc.fr

D. Lechner is with Inrets-MA Laboratory, Departement of Accident Mechanism Analysis, Chemin de la Croix Blanche, 13300 Salon de Provence, France daniel.lechner@inrets.fr

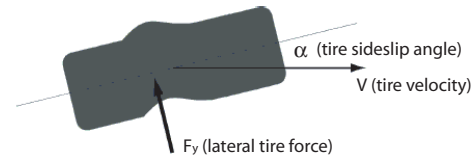


Fig. 1. Lateral tire deformation

is the necessary force to hold a vehicle through a turn. It is generated by the lateral tire deformation in the contact patch, as illustrated in figure 1. The angle of deformation, or the difference between the tire's heading and velocity, is known as the tire slip angle. The tire lateral force is usually represented in function of its sideslip angle. As pictured in figure 2, the general characteristics of the lateral force are that it grows linearly for small slip angles and it ultimately levels off. This phenomenon is due to the limits of tire adhesion. The limits of handling are defined by the maximum available lateral force $\mu_y F_z$, where μ_y is the lateral tire/road friction and F_z is the vertical tire force. When operating in the linear region (lateral acceleration $a_y < 0.4g$), a vehicle responds predictably to the driver's inputs. When a vehicle undergoes high accelerations ($a_y > 0.4g$), or when road friction changes, the vehicle dynamic becomes nonlinear and the force begins to saturate. Consequently, the tire enters the nonlinear operating region and the vehicle approaches its handling limits and its response becomes less predictable.

Lateral vehicle dynamic estimation has been widely dis-

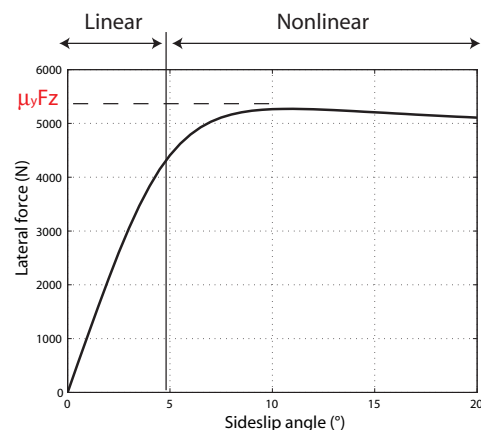


Fig. 2. Generic lateral tire curve

cussed in the literature, and several studies have been

conducted regarding the estimation of the lateral tire-road forces. For example, some studies, like in [2], estimate some dynamic states for a four-wheel vehicle model comprising four degrees DOF. Consequently, the lateral tire forces at each tire are calculated based on the estimated states and using a quasi-static tire model. Ray, in [3], estimates the vehicle dynamic states and the lateral tire forces per front and rear axles for a nine DOF vehicle model. The author uses measurements of the applied wheel torques as inputs to his model. We note that the torque is difficult to get in practice; it requires expensive sensors. More recently, in [4] and [5], authors propose observers to estimate lateral forces per axle without using torque measures. In [3]-[5], lateral forces are modelled with a derivative equal to random noise. The authors in [5] remark that such modeling leads to a noticeable inaccuracy when estimating individual lateral tire forces, but not lateral forces per axle. This phenomenon is due to the non-representation of the lateral load transfer when modeling.

The main goal of this study is to develop an estimation method that uses a simple vehicle-road model and a certain number of valid measurements in order to estimate in real-time and in accurate way the lateral force at each individual tire/road contact point. We assume a prior knowledge or classification of the road surface. This study presents three significant particularities:

- 1) The estimation process does not use the measurement of wheel torques.
- 2) In contrast to many existing approaches which assume constant vertical forces, the lateral forces estimation process presented in this study consider the vertical forces variation. The load at each tire is reconstructed according to the different methods presented in our previous study [6].
- 3) The tire's dynamic behavior is taken into account when evaluating the generated lateral tire force, while the major part of the existing studies use a static tire model.

In order to show the effectiveness of the estimation method, some validation tests were carried out on an instrumented vehicle in realistic driving situations.

The remainder of the paper is organized as follows. Section 2 describes and discusses the vehicle model and the tire/road interaction phenomenon. Section 3 illustrates the observer design and presents the observability analysis. In section 4 the results are discussed and compared to real experimental data, and then in the final section we make some concluding remarks regarding our study and future perspectives.

II. VEHICLE/ROAD MODEL

This section presents the vehicle model and tire/road interaction dynamics, especially the lateral tire forces. Since the quality of the observer largely depends on the accuracy of the vehicle and tire models, the underlying models must be precise. Taking real-time calculation requirements, the models should also be simple.

A. Four-wheel vehicle model

The state estimator presented in this study is based on a Four-Wheel Vehicle Model (FWVM), that comprises three degrees of freedom:

- The motion in the longitudinal direction or longitudinal velocity V_x .
- The motion in lateral direction or lateral velocity V_y .
- The yaw motion around the vertical axis, described by the yaw rate $\dot{\psi}$, with I_z the yaw moment of inertia.

Figure 3 shows the scheme of the FWVM in the longitudinal-lateral plane. This model ignores heave, roll, and pitch motions and has no suspension. The front and rear track widths are assumed to be equal E . Besides, assuming that rear steering angles are approximately null, the direction or heading of the rear tires is the same as that of the vehicle. The heading of the front tires includes the steering angle, δ . The front steering angles are assumed to be equal ($\delta_{11} = \delta_{12} = \delta$).

The sideslip at the vehicle center of gravity (cog), β , is the angle between the velocity vector, V_g , and the true heading of the vehicle, ψ . The longitudinal and lateral forces, $F_{x,y,i,j}$, acting during the movement, are shown for front and rear tires of the vehicle.

While considering the important effect of the longitudinal forces on the lateral ones, its inclusion makes solving the lateral estimation problem considerably more complex. For this reason, some recent studies presented in literature, as in [7], propose to solve the lateral estimation problem in the absence of rough longitudinal forces first and include them in later studies. In this study, we extend this hypothesis, and we suppose a front-wheel drive, where only front axle longitudinal forces are considered, and the rear ones are neglected with respect to the front ones. This can be done by focusing on solving the estimation problem when the vehicle is driven at constant speeds or when the vehicle accelerates or decelerates slowly, avoiding the case of rough braking/acceleration. This is the approach taken throughout this study, and we leave the complete inclusion of longitudinal forces into the estimation problem for future work.

The dynamics of the vehicle can be obtained by summing the forces and moments about the vehicle's center of gravity. Consequently, the simplified FWVM is formulated as the following dynamic relationships:

$$\ddot{\psi} = \frac{1}{I_z} \begin{bmatrix} l_f [F_{y11} \cos \delta + F_{y12} \cos \delta + F_{x1} \sin \delta] \\ -l_r [F_{y21} + F_{y22}] + \frac{E}{2} [F_{y11} \sin \delta - F_{y12} \sin \delta + F_{x12} \cos \delta - F_{x11} \cos \delta] \end{bmatrix} \quad (1)$$

$$\dot{V}_x = V_y \dot{\psi} + \frac{1}{m_v} [-F_{x1} \cos \delta - (F_{y11} + F_{y12}) \sin \delta] \quad (2)$$

$$\dot{V}_y = -V_x \dot{\psi} + \frac{1}{m_v} \begin{bmatrix} (F_{y11} + F_{y12}) \cos \delta + F_{y21} + F_{y22} - F_{x1} \sin \delta \end{bmatrix} \quad (3)$$

$$a_y = \frac{1}{m_v} \begin{bmatrix} F_{y12} \cos \delta + (F_{y21} + F_{y22}) + F_{x1} \sin \delta + F_{y11} \cos \delta \end{bmatrix} \quad (4)$$

$$a_x = \frac{1}{m_v} [-F_{y11} \sin \delta - F_{y12} \sin \delta + F_{x1} \cos \delta] \quad (5)$$

where, m_v is the vehicle mass, a_x is the longitudinal acceleration and F_{x1} is the longitudinal force per the front axle ($F_{x1} = F_{x12} + F_{x12}$).

The longitudinal and lateral velocities, the steer angle of the front wheels and the yaw rate are then used as a basis for the calculation of the tyre slip angles α_{ij} as well as the vehicle

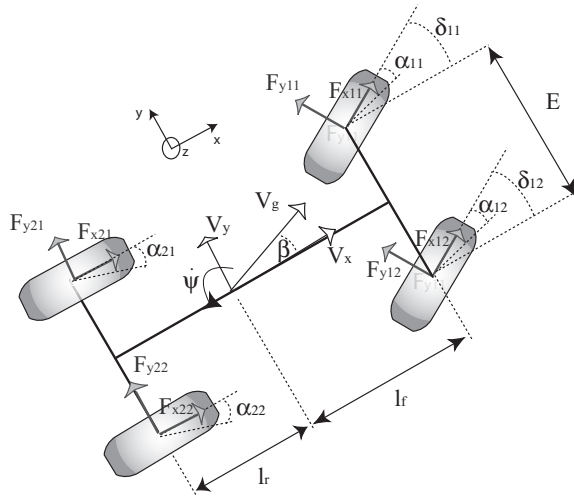


Fig. 3. 2D schema representation of a four-wheel vehicle model

body slip angle β [11]:

$$\alpha_{11} = \delta - \arctan \left[\frac{V_y + l_f \dot{\psi}}{V_x - E \dot{\psi}/2} \right], \quad (6)$$

$$\alpha_{12} = \delta - \arctan \left[\frac{V_y + l_f \dot{\psi}}{V_x + E \dot{\psi}/2} \right], \quad (7)$$

$$\alpha_{21} = -\arctan \left[\frac{V_y - l_r \dot{\psi}}{V_x - E \dot{\psi}/2} \right], \quad (8)$$

$$\alpha_{22} = -\arctan \left[\frac{V_y - l_r \dot{\psi}}{V_x + E \dot{\psi}/2} \right], \quad (9)$$

$$\beta = \arctan \frac{V_y}{V_x}. \quad (10)$$

B. Dynamic tire model representation

The lateral deformation on the tire, that mainly creates the lateral force, does not occur instantaneously following a steer angle input. The time delay (result of the distance delay) for lateral deformation, and consequently lateral force response, is an important transient tire property. This phenomenon is typically characterized by the measurement of the so-called relaxation length.

The combination of the suspension/tyre relaxation length and the quasi-static tire models, allows a better evaluation of the tire's dynamic behavior. The tire dynamic effects by means of an equivalent suspension/tyre relaxation length is formulated using a first-order transient tire model given as [8]:

$$\dot{F}_y = \frac{V_x}{\sigma} (-F_y + \bar{F}_y), \quad (11)$$

where σ is the relaxation length, and \bar{F}_y corresponds to a quasi-static model.

Many different quasi-static tire models are to be found in the literature, based on the physical nature of the tire and/or on empirical formulations deriving from experimental data, such as the Pacejka and Dugoff models [9], [10]. To describe the tire nonlinearity with minimal complexity and qualitative correspondence with experimental tire behavior, we choose

the Dugoff tire model.

Assuming pure slip conditions with negligible longitudinal slip, the simplified version of the Dugoff tire model becomes:

$$\bar{F}_{yij} = -C_{\alpha ij} \tan \alpha f(\lambda), \quad (12)$$

and $f(\lambda)$ is given by:

$$f(\lambda) = \begin{cases} (2 - \lambda)\lambda, & \text{if } \lambda < 1 \\ 1, & \text{if } \lambda \geq 1 \end{cases} \quad (13)$$

$$\lambda = \frac{\mu_y F_{zij}}{2C_{\alpha ij} |\tan \alpha_{ij}|}. \quad (14)$$

where $C_{\alpha}(F_z, \mu_y)$ is the cornering stiffness of the tire. As the longitudinal slips are ignored in this study, the road friction μ is assumed equal to the lateral road friction μ_y .

III. OBSERVER DESIGN

This section presents a description of the observer devoted to lateral tire forces and vehicle's sideslip angle. The state-space formulation, analysis concerning the incorporation of the lateral forces as states, the observability analysis of the system and the estimation method will be presented in the following.

A. Stochastic state-space representation

As the Kalman filter is used for estimating individual lateral tire force and evaluating the sideslip angle, it is necessary to represent the system model in a discrete stochastic state-space form. Combining and discretizing the relations (1)-(14), the model described in the previous section can be formulated as follows:

$$\begin{cases} X_k = f(X_{k-1}, U_k) + w_k \\ Y_k = h(X_k) + v_k \end{cases}, \quad (15)$$

where X_k , U_k , Y_k denote respectively the state, the input and the measurement vectors. The functions $f(\cdot)$ and $h(\cdot)$ represent the states evolution and the observation equations. The state disturbance and the observation noise vector, respectively w_k and v_k are assumed to be gaussian, temporally uncorrelated and zero-mean.

Note that the discretization of equations (1),(2),(3) and (11) is done using the first-order Euler approximation formula. This method is chosen in our study because it is simple and corresponds to real-time implementation requirements.

The state vector X_k , at each instant k , comprises yaw rate, longitudinal and lateral velocities, individual lateral forces and the sum of the front longitudinal tire forces:

$$X_k = [\dot{\psi}_k, V_{x,k}, V_{y,k}, F_{y11,k}, F_{y12,k}, F_{y21,k}, F_{y22,k}, F_{x1,k}]^T \quad (16)$$

Therefore, the sideslip angle at the vehicle's cog can be directly evaluated using equation (10). If the vehicle is at rest ($V_x = 0$), β is assumed equal to zero. The state vector X is initialized as a null vector.

The input vector U_k comprises the steering angle, and the vertical forces considered estimated as presented in our previous work [6]:

$$U_k = [\delta_k, F_{z11,k}, F_{z12,k}, F_{z21,k}, F_{z22,k}]^T \quad (17)$$

The measure vector Y_k comprises the yaw rate, the longitudinal velocity, the longitudinal and the lateral accelerations:

$$Y_k = [\dot{\psi}_k, V_{x,k}, a_{x,k}, a_{y,k}]^T \quad (18)$$

Note that V_x is approximated by the mean of the rear wheel velocities calculated from wheel-encoder data. This approximation is valid for a front steering configuration.

A closer investigation reveals that for the expression for $\ddot{\psi}$ (see equation (1)), the longitudinal tire forces appear to affect the yaw rate not only through the term $F_{x1} \sin \delta$, via the moment arm due to the longitudinal distance of the front axle from the cog. But, in fact, the yaw rate is also affected by the longitudinal tire forces, via the moment arm due to the lateral distance of the wheels from the cog ($E/2$). Basically, a difference in right and left longitudinal forces, $(F_{x12} \cos \delta - F_{x11} \cos \delta)$, generates a yaw torque on the car. However F_{x11} and F_{x12} cannot be considered separately as states in the vector X for observability reasons. To face this problem, we admit the assumption proposed by [4], where the longitudinal tire forces and force sums are associated according to the dispersion of vertical forces:

$$F_{x11} = \frac{F_{z11}}{F_{z12} + F_{z11}} F_{x1}, \quad F_{x12} = \frac{F_{z12}}{F_{z12} + F_{z11}} F_{x1}. \quad (19)$$

Considering the proposed X , U and Y vectors, the nonlinear functions $f(\cdot)$ and $h(\cdot)$ representing the state and the observation equations are calculated according to equations (1)-(14) and (19).

B. Analysis and observation

In this subsection, we make some analysis and observations regarding the introduction of the tire forces as system states, where their dynamics are described by the relaxation-length concept. This consideration allows:

- a better evaluation of the tire forces. In fact, whatever the complexity of the tire models, there are several reasons why such models do not match the actual tyre forces perfectly [12]. From these reasons, we can cite especially the changes in the tire's pressure and temperature and the changes in the road characteristics. Therefore, we believe that according to the closed loop observer theory, the integration of the tire forces in the state vector may lead to better results than just using an open loop tire model.
- a better understanding of the tire behaviors using the relaxation-length formulation, especially in transient maneuvers [13].
- the forces reconstruction to be done robustly with respect to some parameter variations. In fact, it is well known that the Kalman filters have proven to be robust to parameter changes.

Taking these observations in mind, one can infer the contribution of this study with respect to others existing studies in the literature like [2], which estimate dynamic variables of the vehicle, and then assess the tire forces using a properly adjusted tire model.

C. Observability analysis

Observability is a measure of how well the internal states of a system can be inferred from knowledge of its inputs and external outputs. This property is often presented as a rank condition on the observability matrix.

Using the nonlinear state-space formulation of the system described above, the observability definition is local and uses the Lie derivative [14]. The corresponding obtained expressions are very complicated, and are not reported in this study. It was deduced that the system is observable except when the vehicle is at rest ($V_x = V_y = 0$) or driven at low velocities. In fact, in these cases, the relaxation tire model is not valid [8]. Moreover, the sideslip angle at the the cog can not be evaluated (see equation (10)). For these situations, we assume that the lateral forces and the sideslip angle are null, which approximately correspond to the real cases (neglecting suspension kinematics).

D. Estimation technique

The aim of an observer or a virtual sensor is to estimate a particular unmeasurable variable from available measurements and a system model in a closed loop observation scheme, as illustrated in figure 4. At each iteration, the state vector is first calculated according to the evolution equation and then corrected online with the measurement errors (innovation) and filter gain K in a recursive prediction-correction mechanism. Due to the nonlinearity of the presented vehicle/tire model, the observer gain is calculated using the Extended Kalman filter method (EKF). The EKF is a set of mathematical equations and is widely represented in [15].

EKF algorithm:

Consider the general discrete nonlinear system:

$$\begin{cases} X_{k+1} &= f(X_k, U_k) + w_k \\ Y_k &= h(X_k) + v_k \end{cases}, \quad (20)$$

where $X_k \in R^n$ is the state vector, $U_k \in R^r$ is the known input vector, $Y_k \in R^m$ is the output vector at time k . The state disturbance and the observation noise vector, respectively w_k and v_k are assumed to be gaussian, temporally uncorrelated and zero-mean:

$$w_k \sim N(0, Q_k), \quad v_k \sim N(0, R_k), \quad (21)$$

where Q and R are the covariance matrices, describing the second-order properties of the state and measurement noises. The EKF can be expressed as follows:

Initialization

$$\begin{cases} \bar{X}_0 &= E[X_0] \\ P_0 &= E[(X_0 - \bar{X}_0)(X_0 - \bar{X}_0)^T] \end{cases} \quad (22)$$

where \bar{X}_0 and P_0 are respectively the initial state and the initial covariance.

Time Update:

$$\begin{cases} \bar{X}_{k|k-1} &= f(\bar{X}_{k-1}, U_k) \\ P_{k|k-1} &= A_k P_{k-1} A_k^T + Q \end{cases} \quad (23)$$

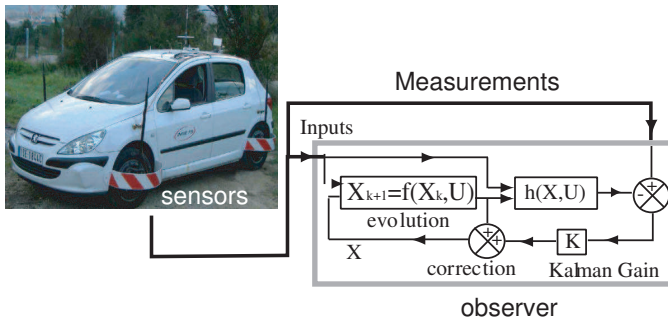


Fig. 4. Process estimation diagram

Measurement update

$$\begin{cases} K_k &= P_{k|k-1} H_k (H_k P_{k|k-1} H_k^T + R)^{-1} \\ \bar{X}_k &= \bar{X}_{k|k-1} + k_k (Y_k - h(\bar{X}_{k|k-1})) \\ P_k &= (I - k_k H_k) P_{k|k-1} \end{cases} \quad (24)$$

where A_k and H_k are respectively the process and measurement Jacobians, P_k is the covariance matrix and K_k is the filter gain at step k .

Observer tuning:

We remember that the computation of the Kalman gain is a subtle mix between process and observation noises. The less noise in the operation compared to the uncertainty in the model, the more the variables will be adapted to follow measurements.

Since the lateral forces are modeled using a relaxation model based on reliable tire models, the uncertainty we put on them is not too high. However, the longitudinal force per front axle is not modeled at all, hence, it is represented by a high noise level. The other states (yaw rate, longitudinal and lateral vehicle velocity) are modeled using the vehicle's equations. Therefore, they are said to have an average noise. On the other hand, since the embedded sensors have good accuracy, the noises on the measurements are quite small. In order to reduce the complexity of the problem, both measurement covariance matrix and the process covariance matrix are assumed to be constant and diagonal. The off-diagonal elements are set to 0.

IV. EXPERIMENTAL EVALUATION

In this section, we present the experimental car used to test the observer's potential. Moreover, we discuss and analyze the test conditions and the observer results.

A. Laboratory car

The experimental vehicle shown in figure 4 is the INRETS-MA (Institut National de la Recherche sur les Transports et leur Sécurité - Département Mécanismes d'Accidents) Laboratory's test vehicle. The vehicle parameters are given in table I. It is a Peugeot 307 equipped with a number of sensors including accelerometers, gyrometers, steering angle sensors, linear relative suspension sensors, three Correbits and four dynamometric wheels.

One Correbit is located in chassis rear overhanging position

Symbol	Value	Unit	Meaning
m_v	1588	kg	vehicle mass
l_f	1.16	m	distance COG-front axle
l_r	1.45	m	distance COG-rear axle
E	1.5	m	track's width
I_z	2395	$kg.m^2$	yaw moment of inertia

TABLE I

NORMALIZED ERRORS BETWEEN ESTIMATIONS AND MEASUREMENTS.

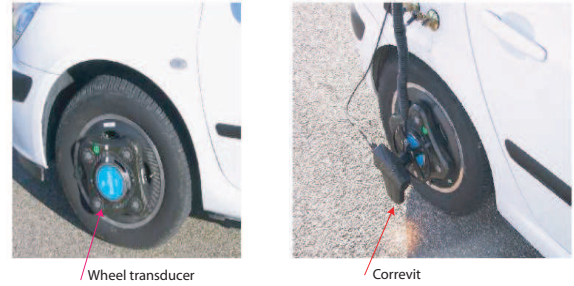


Fig. 5. Wheel-force transducer and sideslip sensor installed at the tire level.

and it measures longitudinal and lateral vehicle speeds and two Correbits are installed on the front right and rear right tires and they measure front and rear tires velocities and sideslip angles. The dynamometric wheels fitted on all four tires, which are able to measure tire forces and wheel torques in and around all three dimensions. We note that the correbit and the wheel-force transducer (see figure 5) are very expensive sensors. The sampling frequency of the different sensors is 100 Hz. For more details concerning the experimental car hardware/software equipments, the reader may refer to [16].

The estimation process algorithm is a computer program written in C++. It is integrated into the laboratory car as a DLL (Dynamic Link Library) that functions according to the vehicle's software acquisition system.

B. Test conditions

To assess the performance of the proposed observer in realistic driving situations, we report a Slalom transient maneuver generated by a sinusoidal steering input. The test is done on dry road (we suppose that $\mu = 1$). This is a difficult maneuver from the estimation viewpoint, because the vehicle dynamics is largely and fastly solicited. With this kind of path, the applied lateral acceleration depends on the steering input.

Steer angle, yaw rate and lateral acceleration are assumed to be the main variables that characterize the lateral dynamics of the vehicle in terms of transient/steady-state response. Figure 6 illustrates the time history of the maneuver as well as the "g-g" acceleration diagram during the course of the test. The circle with radius equal to 0.4g, drawn in the "g-g" diagram, separates the linear and nonlinear region of handling. In fact, if accelerations fall inside the circle, then we are in normal driving conditions. Otherwise, the vehicle reaches the

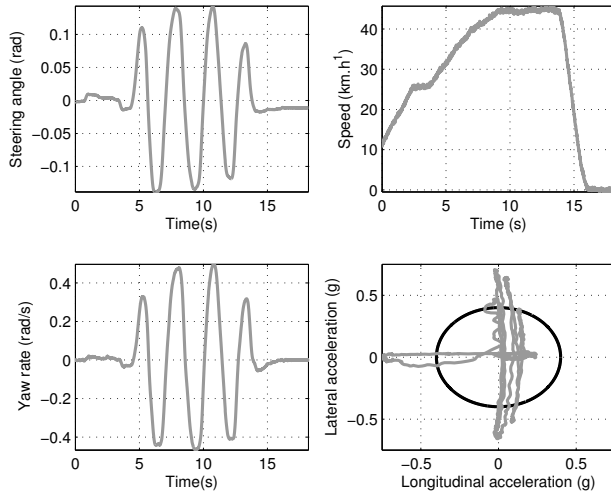


Fig. 6. Slalom test: steering angle, vehicle's speed, yaw rate and "g-g" acceleration diagram.

nonlinear handling behavior. Looking to this "g-g" diagram, we can deduce that large lateral accelerations were obtained during the test (absolute value up to 0.55g). This means that the experimental vehicle was put in a critical driving situation.

C. Observer evaluation

The observer results are presented in two forms: as tables of normalized errors, and as figures comparing the measurements and the estimations. The normalized error for an estimation z is defined as:

$$\epsilon_z = 100 \times \frac{\|z_{obs} - z_{measured}\|}{\max(\|z_{measured}\|)} \quad (25)$$

where z_{obs} is the variable calculated by the observer, $z_{measured}$ is the measured variable and $\max(\|z_{measured}\|)$ is the absolute maximum value of the measured variable during the test maneuver.

Figures 7 and 8 show a comparison of the measured lateral forces and the estimated ones. Figure 9 depicts the estimates of the sideslip angle. It is seen that the estimation errors are practically acceptable.

This maneuver can be decomposed in three parts, and it is interpreted as follows:

- For $(0s < t < 4s)$, the vehicle drives in a straightline and accelerates with $a_x \approx 0.2g$. There is no lateral acceleration signal registered during this time. Consequently, the lateral forces and sideslip angle observed are null. Again, we believe that the lateral forces measured by the dynamometer during this time window, are due to the suspension geometries (camber angle, ... [17]) and not to sideslip angle. Therefore, they cannot be observed by the proposed estimator.

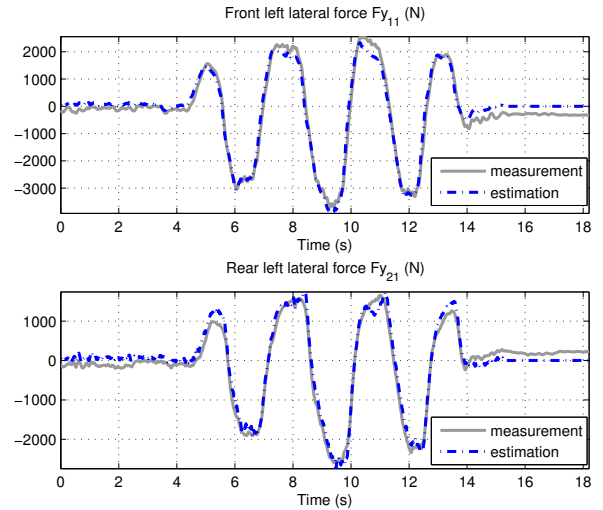


Fig. 7. Estimation of the left-hand lateral tire forces.

- Second, the car negotiates a pure 0.5 Hz slalom at a constant moderate speed of around 12 m/s. This maneuver intermittently enters the nonlinear operating region of the tires (near $t = 6s, 8s, 9s, 11s$ and $12s$). High lateral forces $[3000 (N) - 4000 (N)]$ are registered during this test. Globally, the observer performs well. However, some errors have to be noted, especially for front tires. We believe that these differences are due to the suspension kinematics and geometries that intervene in this severe and fast maneuver. During this time period, it is clear that the sideslip angle closely tracks the Correvit sensor's measure.

A closer investigation reveals that, at each instant, the lateral forces recorded by the compressed tires are much higher than forces generated by the reveal ones. This phenomenon is due to the high amount of load that moves from the left to the right side when the vehicle rolls during slaloming. In fact, as can be seen from Dugoff's formula, the lateral force developed by a tire increases as the applied vertical force increases.

- Finally for $t > 14s$, the car stops slaloming, decelerates with $a_x \approx 0.6g$ and then stops. This phase is similar to the first one.

The experimental slalom maneuver demonstrates that the speed of the observers is adequate for satisfactory characterization of the tire lateral force during fast steering maneuvers. Table II that represents the normalized mean and standard deviation errors between measurements and estimations, confirm the observer efficiency with acceptable errors.

V. CONCLUSION

This paper presents a new method for estimating the lateral tire/road forces and the vehicle's sideslip angle, that is to say, variables among the most important ones affecting vehicle

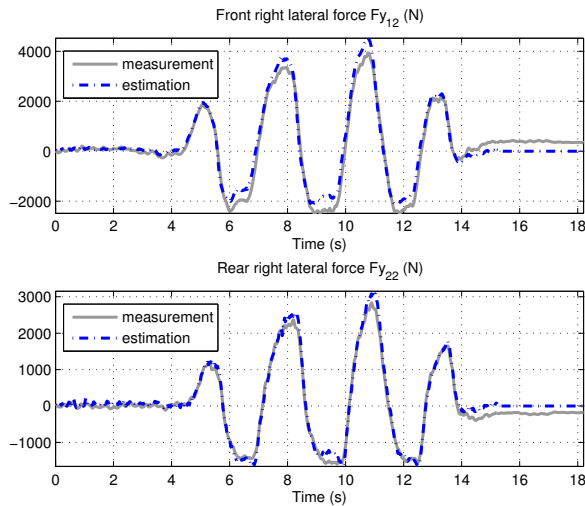


Fig. 8. Estimation of the right-hand lateral tire forces.

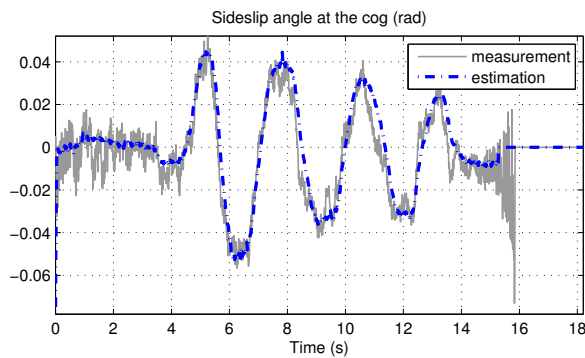


Fig. 9. Estimation of the sideslip angle at the cog.

stability.

The results from the estimation process are very promising. A comparison with real experimental data demonstrates the potential of the estimation process. This is one of the important results of this work. Another important result concerns the estimation of individual lateral forces acting on each tire. This can be seen as an advance with respect to the current vehicle-dynamics literature.

Note that, in the frame work of the national french PREDIT/SARI/RADARR project, the proposed observer was tested in a multitude of situations (lane change, double lane change, randabout,...) at high speeds (up to 110 km/h). The tests were carried out on different dry roads with different characteristics, and the results were always satisfactory with normalized errors $< 8\%$.

Future studies will improve the vehicle/road model in order to widen validity domains for the presented observer, and make it adaptative with the road conditions (especially the road friction). Moreover, the effect of coupling vertical/longitudinal/lateral dynamics can be a crucial point that deserves to be studied.

	Max	Mean %	Std %
F_{y11}	3715 (N)	7.23	6.80
F_{y12}	3941 (N)	10.22	8.74
F_{y21}	2596 (N)	7.51	5.52
F_{y22}	2833 (N)	7.44	6.77
β	0.05 (rad)	5.32	5.41

TABLE II

NORMALIZED ERRORS BETWEEN ESTIMATIONS AND MEASUREMENTS.

REFERENCES

- [1] Y. Hsu and J. Chistian Gerdes, *Experimental studies of using steering torque under various road conditions for sideslip and friction estimation*, Proceedings of the 2007 IFAC Symposium on Advances in Automotive Control, Monterey, California, 2007.
- [2] J. Dakhlallah, S. Glaser, S. Mammam and Y. Sebsadji, *Tire road forces estimation using extended Kalman filter and sideslip angle evaluation*, Proceedings of the 2008 American Control Conference, Washington, USA, June 2008.
- [3] L. R. Ray, *Nonlinear tire force estimation and road friction identification: simulation and experiments*, Automatica, volume 33, no. 10, pages 1819-1833, 1997.
- [4] G. Baffet A. Charara, D. Lechner and D. Thomas, *Experimental evaluation of observers for tire-road forces, sideslip angle and wheel cornering stiffness*, Vehicle System Dynamics, volume 45, pages 191-216, june 2008.
- [5] M. A. Wilkin, W. J. Manning, D. A. Crolla, M. C. Levesley Use of an extended Kalman filter as a robust tyre force estimator, Vehicle System Dynamics, volume 44, pages 50-59, 2006.
- [6] M. Doumiati, A. Victorino, A. Charara, D. Lechner and G. Baffet, *lateral load transfer and normal forces estimation for vehicle safety: experimental evaluation*, Vehicle System Dynamics (to appear).
- [7] R. Rajamani, *Estimation and control of lateral tire forces using steering torque*, Ph. D, Stanford University, USA, 2009.
- [8] R. Rajamani, *ehicle dynamics and control*, Springer, 2006.
- [9] Hans B. Pacejka, *Tyre and vehicle dynamics*, Elsevier, 2002.
- [10] J. Dugoff, P. Fanches and L. Segel, *An analysis of tire properties and their influence on vehicle dynamic performance*, SAE paper (700377), 1970.
- [11] U. Kiencke and L. Nielsen, *Automotive control systems*, Springer, 2000.
- [12] L. Lidner, *Experience with the magic formula tyre model*, Proceedings of the 1st International Colloquium on Tyre Models for Vehicle Dynamic Analysis, Amsterdam, Holland, 1991.
- [13] J. Svendenius, *Tire modeling and friction estimation*, PhD thesis, Lund University, Sweden, 2007.
- [14] H. Nijmeijer and A.J. Van der Schaft, *Nonlinear dynamical control systems*, Springer Verlag, 1991.
- [15] B. Ristic, S. Arulampalam and N. Gordon, *Beyond the Kalman filter*, Artech House, 2004.
- [16] D. Lechner, *Embedded laboratory for vehicle dynamic measurements*, 9th International symposium on advanced vehicle control, Kobe, Japan, Octobre 2008.
- [17] W.F. Milliken and D.L. Milliken, *Race car vehicle dynamics*, Society of Automotive Engineers, Inc, U.S.A, 1995.